Image-based Battery Health Monitoring for Capacity Degradation Analysis

Ji Young Yun * **Haechang Kim** * **Jong Min Lee** *†

* *Department of Chemical and Biological Engineering, Institute of Chemical Process, Seoul National University, Seoul, 08826, Korea (email: jongmin@snu.ac.kr).*

Abstract: Accurate battery health prediction is crucial for prolonging battery life and ensuring safety. Traditional methods relying on raw time-series data struggle with complex temporal patterns and sensor noise. To address these limitations, we propose a novel approach that utilizes image-transformed data to perform "knee classification" and State of Health (SOH) estimation concurrently. This integrated approach detects aging events and continuously monitors SOH, enabling preemptive interventions. We employ a Convolutional Neural Network (CNN) to simultaneously perform knee classification and SOH estimation, incorporating Gradient-weighted Class Activation Mapping (Grad-CAM) to enhance interpretability by emphasizing critical regions involved in the classification process. The proposed model achieves an 89% classification accuracy, with higher recall than the time-series-based approach, particularly in identifying the intermediate state. Additionally, the pre-trained CNN-based model attains an R^2 value of 0.977 in SOH prediction, demonstrating its effectiveness for battery condition monitoring. These findings highlight the benefits of an integrated multi-task learning approach, addressing the limitations of conventional time-series models.

Keywords: Lithium-ion batteries, Knee-onset, Knee-point, State of Health, Recurrence plot, Convolutional neural network, Gradient-weighted Class Activation Mapping

1. INTRODUCTION

Lithium-ion batteries (LIBs) are of paramount importance in a multitude of applications, including electric vehicles (EVs), electronic devices, and energy storage systems (ESSs), due to their elevated energy density and extended lifespan. Nevertheless, recurrent charge and discharge cycles inevitably result in degradation, which is characterized by capacity loss, augmented internal resistance, and diminished overall performance. These changes significantly impact battery life and highlight the need for real-time monitoring and accurate health prediction to ensure reliable and efficient maintenance.

The principal metrics for evaluating battery health are State of Health (SOH) and Remaining Useful Life (RUL). However, SOH and RUL each have limitations in detecting preliminary signs of capacity loss. While SOH provides a snapshot of the battery's current state, it cannot forecast the decay rate. RUL focuses on the remaining service life, which can be insufficient for examining the root causes of capacity fade.

To address this issue, the concepts of the "knee-point" and "knee-onset" have been introduced as key indicators of battery efficiency reduction. The knee-point refers to the transition point where capacity begins to decrease rapidly, representing a pivotal stage in the decay process (Attia et al. (2022)). Conversely, the knee-onset marks the initial point at which capacity fade becomes non-linear, indicating when linear approximation can no longer adequately describe degradation (Fermín-Cueto et al. (2020)). Both points are closely associated with the aging progression, making their accurate estimation essential for robust battery life prediction and management. In particular, recognition of the knee-onset enables preventive measures to mitigate damage or safety risks before significant degradation occurs.

Recent studies have employed data-driven approaches to predict health indicators. These methods leverage large datasets to gain insights into battery functional state, effectively replacing traditional physics-based models. For instance, Greenbank and Howey (2021) adopted Gaussian Process Regression (GPR) to improve model performance in predicting rapid capacity degradation and end-of-life. In a similar vein, Zhang et al. (2018) and Zhang et al. (2023) utilized Long Short-Term Memory (LSTM) for RUL and SOH prediction, respectively, thereby incorporating long-term dependencies in their respective methodologies. Additionally, Sohn et al. (2022) introduced a Convolutional Neural Network (CNN)-based knee-point prediction model, while Ren et al. (2020) combined CNN and LSTM to develop an RUL prediction model that incorporates both temporal characteristics and data patterns.

However, existing studies encounter limitations in model performance when utilizing time-series data in its original form, as this frequently fails to capture complex temporal patterns and remains susceptible to sensor noise. Moreover, task-specific models often struggle to acquire generalized data representations, thereby constraining their generalizability across diverse tasks or as pre-trained models for more extensive applications.

We propose a novel battery health monitoring method that uses image-transformed data for capacity degradation analysis. The image representation of time-series data is capable of encapsulating the necessary information on degradation patterns while filtering out noise. The proposed methodology employs a CNN structure, leveraging its capability to effectively extract spatial features from the transformed image data. Such characteristics enable the identification of knee points and accurate estimation of SOH. Additionally, the prediction outcomes are analyzed through Gradient-weighted Class Activation Mapping (Grad-CAM), which visually highlights influential regions, providing a certain level of interpretability for domain experts. Consequently, our approach contributes to improved battery durability and safety management.

The structure of this paper is as follows: Section 2 describes the data analyses, model architecture, and overall framework. Section 3 presents and analyzes classification and SOH estimation results based on the proposed method. Finally, Section 4 concludes with insights from the study and outlines directions for future research.

2. METHODS

2.1 Dataset

The dataset from Severson et al. (2019) was utilized in this study. The dataset encompasses charge-discharge cycle data for commercial lithium-ion batteries (LFP/graphite cells, A123 Systems) subjected to fast-charging conditions. It comprises 124 cells, each cycled until reaching 80% of its rated capacity using either a one-stage or two-stage fast-charging protocol. The average charge rates ranged from 3.6C to 6C, with all cells discharged at a rate of 4C. Each cell has a rated capacity of 1.1 Ah and a nominal voltage of 3.3 V, and voltage, current, temperature, and internal resistance are recorded for each cycle.

2.2 Data Preprocessing

The input data consists of voltage (V), current (I), and temperature (T) measurements obtained during the charge-discharge process. Initially, Discrete Wavelet Transform (DWT) was performed for noise reduction, as it is well-suited for time-series data by enabling multi-resolution analysis (Mallat (1989)). This method effectively suppresses high-frequency noise while preserving both local variations and global trends in the V, I, and T signals. To address variations in data length and missing time points, interpolation was applied to standardize each cycle to 256 time steps.

The knee-point and knee-onset for each cell were calculated using the Bacon-Watts model and the double Bacon-Watts model, as proposed in Fermín-Cueto et al. (2020). The Bacon-Watts model is a method for approximating capacity degradation with two linear functions, as given in Eq. (1). In this model, the slopes of the linear segments α_1 and α_2 and the transition point c_1, indicating the knee-point, were adjusted to align with the capacity fade curve.

$$Q = \alpha_0 + \alpha_1(c - c_1) + \alpha_2(c - c_1)\tanh\left\{\frac{c - c_1}{\gamma}\right\} + Z \tag{1}$$

To determine the knee-onset location, the double Bacon-Watts model with two transition points (c_0 and c_2) was implemented, where c_0 denotes the knee-onset, as defined in Eq. (2).

$$\begin{aligned} Q = \alpha_0 + \alpha_1(c - c_0) + \alpha_2(c - c_0)\tanh\left\{\frac{c - c_0}{\gamma}\right\} \\ +\alpha_3(c - c_2)\tanh\left\{\frac{c - c_2}{\gamma}\right\} + Z \end{aligned} \tag{2}$$

These models enabled the determination of both the knee-onset and knee-point while accounting for the degradation pattern of each cell, ensuring a consistent optimization approach across all cases. Based on these values, each cycle was labeled for classification, a process defined as "knee classification." Specifically, the data before the knee-onset was labeled as 0, the interval between the knee-onset and knee-point as 1 (specified as "Between point"), and the remainder after the knee-point as 2.

2.3 Recurrence Plot Transformation

V, I, and T time-series data were converted into images to capture subtle variations during battery charging and discharging cycles effectively. Representing the data as images has been confirmed to enrich potential information by visually revealing critical patterns, as demonstrated in Garcia et al. (2022).

This study employed the Recurrence Plot (RP) method, as outlined in Eckmann et al. (1995), due to its computational efficiency and its ability to capture the evolution of patterns over time. The RP calculates similarity based on the spatial distance between specific points in the data trajectory, effectively characterizing the dynamic properties of the underlying patterns.

Traditionally, recurrence is calculated using a binary scheme based on a predefined threshold, simplifying all recurrence measures to either 0 or 1. In contrast, the proposed approach preserves the original recurrence values when they fall below the threshold. This refinement enhances sensitivity to subtle variations in battery conditions by maintaining temporal details, while concurrently reducing noise through threshold-based filtering of larger distances. The recurrence $R_{i,j}$ between time points i and j can be calculated as Eq. 3:

$$R_{i,j} = \begin{cases} \|\mathbf{x}_i - \mathbf{x}_j\|, & \text{if } \|\mathbf{x}_i - \mathbf{x}_j\| \le \varepsilon \\ 0, & \text{otherwise} \end{cases} \tag{3}$$

where $\mathbf{x}_i$ and $\mathbf{x}_j$ mean 3-dimensional vectors composed of V, I, and T at each time point.

Given that V and I are tightly coupled and T is integrally linked despite its delayed response, these features exhibit coordinated behavior during battery operation. Consequently, we integrated them into a single grayscale image rather than processing each channel separately, enabling the CNN model to effectively capture their joint dynamics.

2.4 Model architecture

A CNN is highly effective for extracting visual features by learning patterns in image data. The convolutional layer is designed to capture local patterns, while the max-pooling layer consolidates these patterns at a global level to preserve key image information. Based on these strengths, this study adopted CNN as the base model to extract essential patterns from time-series images.

The CNN model architecture implemented in this study is illustrated in Fig. 1, with the parameters for each layer delineated in Table. 1. The model extracts high-level image features incrementally through multiple convolutional and pooling layers, concluding with knee class in the final fully connected layer.

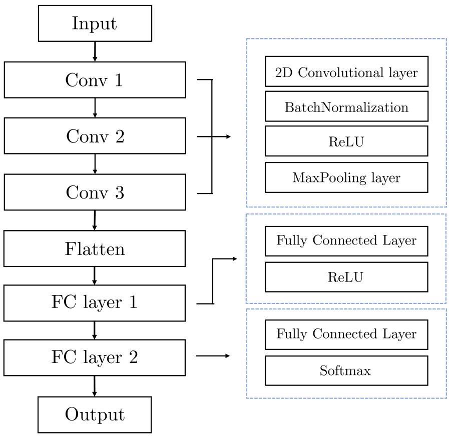

Fig. 1. CNN model architecture

Table 1. Model parameters

Layer Name	Kernels	Nodes	Kernel size/Stride
Input	-	-	-
Convolutional Layer 1	16	-	3/1
Max Pooling Layer 1	-	-	2/2
Convolutional Layer 2	32	-	3/1
Max Pooling Layer 2	-	-	2/2
Convolutional Layer 3	64	-	3/1
Max Pooling Layer 3	-	-	2/2
Fully Connected Layer 1	-	256	-
Fully Connected Layer 2	-	3	-

In knee classification, the cross-entropy loss function was applied to impose penalties on incorrect predictions and enhance the model's capacity to discern features.

$$\text{Cross Entropy} = -\frac{1}{N}\sum_{i=1}^{N}\sum_{c=1}^{C} p_{i,c}\log(q_{i,c}) \tag{4}$$

where N is the number of data points, C is the number of classes, $p_{i,c}$ is a one-hot encoded vector that equals 1 if the true class is c and 0 otherwise, and $q_{i,c}$ is the predicted probability that the i^{th} data point belongs to class c.

In addition, the SOH prediction task was executed using a pre-trained model, for which Mean Squared Error (MSE) loss was deployed to enhance the continuous value prediction accuracy. Minimizing the MSE between predicted $(\hat{y}_i)$ and actual (y_i) values ensures accurate estimation of SOH.

$$\text{MSE} = \frac{1}{N}\sum_{i=1}^{N}(y_i - \hat{y}_i)^2 \tag{5}$$

2.5 Model explanation

We utilized Grad-CAM to interpret the behavior of the CNN model. By leveraging gradient information from the feature map in the final convolutional layer of CNN, Grad-CAM can visualize crucial regions that contribute significantly to the prediction of each class.

In Grad-CAM, each filter k is assigned a weight α_k^c, reflecting its contribution toward predicting class c. The weight is determined based on the gradient of the class prediction score y^c with respect to the feature map A^k, as follows:

$$\alpha_k^c = \frac{1}{Z}\sum_i\sum_j \frac{\partial y^c}{\partial A_{ij}^k} \tag{6}$$

where Z denotes the total number of elements in the feature map, and $\frac{\partial y^c}{\partial A_{ij}^k}$ quantifies the influence of the feature map at location (i, j) on the prediction score for class c.

The final Grad-CAM map $L_{\text{Grad-CAM}}^c$ is then computed using the following equation:

$$L_{\text{Grad-CAM}}^c = \text{ReLU}\left(\sum_k \alpha_k^c A^k\right) \tag{7}$$

The ReLU function filters out negative values, ensuring that only the most critical areas highlighted by the model are visualized. Through Grad-CAM analysis, we gain insights into critical time steps and temporal patterns that substantially influenced the model's decisions.

2.6 Overall Framework

The overall battery health monitoring framework is illustrated in Fig. 2. Initially, the battery cycle data (V, I, T) were transformed into RP-based images to capture temporal degradation patterns efficiently. The CNN model was trained on these images to perform knee classification, with labels derived from the Bacon-Watts and double Bacon-Watts models. Subsequently, Grad-CAM analysis was conducted to identify regions in the images that significantly influenced the model predictions. Finally, the pre-trained CNN was fine-tuned for SOH estimation to demonstrate its generalized predictive capability.

3. RESULTS AND DISCUSSION

3.1 Data processing results

Fig. 3 illustrates the knee-onset and knee-point identified from the capacity degradation curve of cell b1c24 in the A123 dataset. The knee-onset appears around cycle 600, where the curve's curvature increases. The knee-point occurs near cycle 750, marking the start of rapid capacity fading. Three representative cycles were selected to capture distinct aging phases. Cycle 100 represents stable conditions before the knee-onset, cycle 650 corresponds to the transition phase between the knee-onset and knee-point, and cycle 1000 reflects conditions following the knee-point.

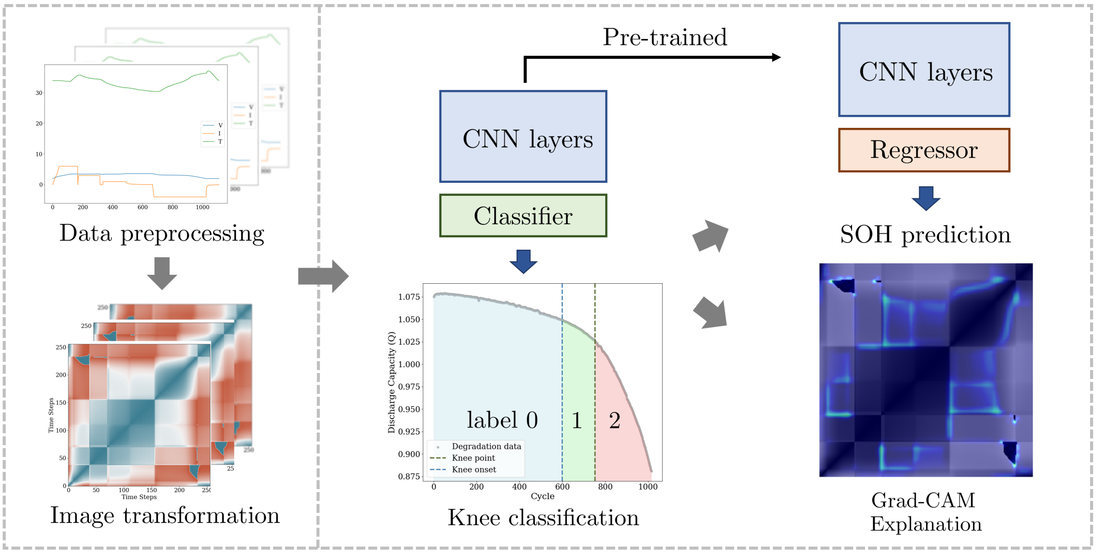

Fig. 2. Overall framework of time-series image-based battery health monitoring

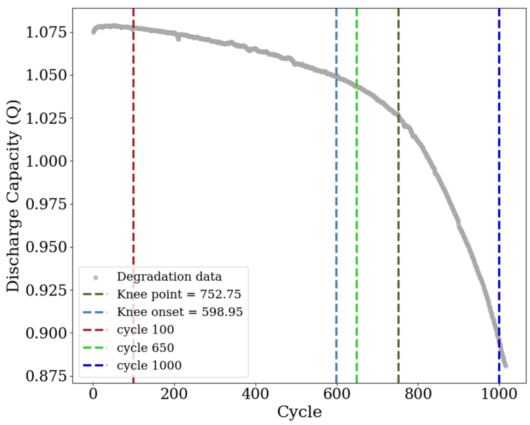

Fig. 3. Identification of knee-onset and knee-point for the sample cell b1c24 in the A123 dataset.

Fig. 4 presents RPs corresponding to these selected cycles. The threshold for generating RPs was set to the top 1% of recurrence values in each cycle. In Fig. 4(a), representing conditions before the knee-onset, a regular diagonal structure is observed. Conversely, Fig. 4(b), representing the phase after the knee-onset, shows a weakened diagonal pattern, particularly around time steps 50 to 150. A notable change in the diagonal structure occurs in Fig. 4(c), with increased regions of high distance values in the early time steps. These visual shifts in the RP indicate changes in the operating state. Specifically, decreasing similarity between time steps suggests a transition toward instability. Similar RP patterns have been observed across cells under various experimental conditions, demonstrating the potential for generalized battery degradation analysis.

3.2 Knee classification results

The 124 cells were divided into 88 cells for training, 23 cells for validation, and 13 cells for testing. The model was trained with the Adam optimizer with a learning rate of 0.001 and a batch size of 128 for up to 100 epochs. Early stopping was implemented, stopping training if the validation loss showed no improvement for 5 consecutive epochs.

The results of knee classification using RP images on the test dataset are summarized in Table 2. The model achieved an overall accuracy of 89%, with a weighted F1 score and a recall of 0.89.

Table 2. Result of knee classification model

Class	**Precision**	**Recall**	**F1 Score**	**Support**
Before knee-onset	0.95	0.93	0.94	6236
Between point	0.63	0.76	0.69	1713
After knee-point	0.92	0.97	0.94	2279
Accuracy			0.89	10228
Macro avg	0.84	0.87	0.85	10228
Weighted avg	0.90	0.89	0.89	10228

Fig. 5 (a) and (b) present the confusion matrices for the RP image-based model and the raw time-series model, respectively. To compare model performance, a 1D CNN model was implemented using raw time-series data as input. The RP image-based model achieved a recall of 0.76 for the intermediate state labeled "between point" (class 1), which occurs between knee-onset and knee-point. In comparison, the model using raw time-series data showed lower performance, with a recall of 0.63 for the same class. In contrast, both models performed well in classifying "before knee-onset" (class 0) and "after knee-point" (class 2).

The difference in classification performance between the RP image-based model and the raw time-series model arises from differences in feature extraction. The time-series model relies on absolute values, making it highly sensitive to changes in data distribution. Although normalization is applied, discrepancies between training and test data still influence predictions. When unseen data deviates from the learned range, the model's ability to generalize diminishes.

In contrast, RP images capture the temporal dynamics within each cycle, creating a structured representation that remains consistent across different datasets. By focusing on relative changes rather than absolute values,

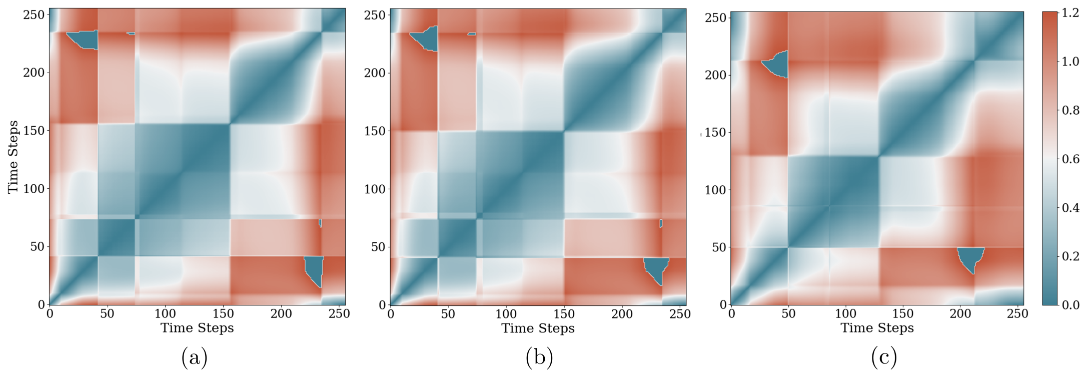

Fig. 4. Recurrence plot transformation of the cell b1c24 in the A123 dataset. (a) cycle 100. (b) cycle 650. (c) cycle 1000.

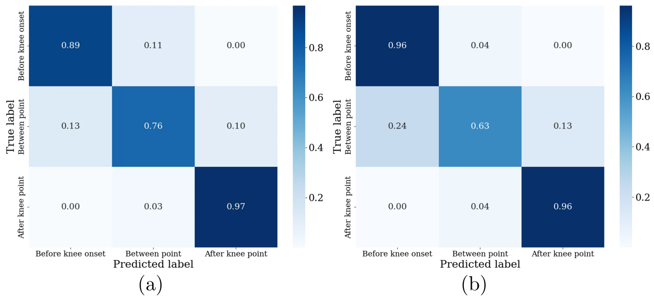

Fig. 5. Confusion matrices of knee classification

this approach reduces the impact of scaling variations. As a result, the RP image-based model exhibits greater robustness, particularly in classifying the intermediate state where data are more limited. These results imply that the RP-based approach improves model stability and generalization. By capturing consistent patterns within each cycle, it reduces sensitivity to distribution shifts, enabling reliable classification across various datasets.

Despite this advantage, class 1 remains difficult to classify due to data imbalance. The limited number of samples reduces the model's ability to learn distinct characteristics, leading to lower recall.

3.3 Grad-CAM analyses

The visualization of the patterns recognized by the model during the knee classification process, using Grad-CAM on cycles from cell b1c24, is shown in Fig. 6.

Fig. 6 (a) presents the Grad-CAM results for cycle 100. At this stage, activation is distributed throughout the image, with relatively high intensity in the vicinity of the diagonal. This observation indicates that the model identifies the 'initial state' based on minor boundary variations and overall stability across different regions. In the initial cycles, features are distributed uniformly, and the model primarily relies on the stability of the overall pattern as a classification criterion.

In Fig. 6 (b), the Grad-CAM results at the 650th cycle are shown. At this stage, activation becomes more concentrated in specific local regions, while overall intensity tends to decrease. This suggests a transitional phase where the initial stable pattern gradually deteriorates after the knee-onset, giving way to emerging degradation characteristics.

It is noteworthy that activation in the upper left and lower right regions highlights features common to both class 0 and class 2, which may contribute to the model's difficulty in clearly distinguishing this cycle.

As illustrated in Fig.6 (c), the Grad-CAM results at the 1000th cycle exhibit prominent activation in the upper left and lower right regions, with faint activation along the diagonal. This suggests that as degradation progresses, irregular and weak patterns become more dominant on the RP, replacing distinct boundaries. A similar trend is observed in Fig. 4 (c), where the recurrence boundaries appear significantly less defined compared to the initial stage, indicating that this change is also reflected in the Grad-CAM activation patterns.

The results of the Grad-CAM analysis provide a visual representation of the features learned by the model that can be used to identify the progression of battery degradation. In the early phase, the uniformity of the overall pattern is the predominant classification criterion. In the subsequent stage, subtle changes associated with degradation become more prominent. In the later stage, the model relies on less distinct and weaker features for classification, as opposed to clear patterns. This implies that Grad-CAM can help explain how the model learns and leverages characteristic patterns of battery degradation.

3.4 SOH prediction results

To evaluate whether the framework developed in this work has learned more generalized properties of battery status, SOH prediction is performed using a pre-trained CNN. The convolutional layer from the CNN model trained for knee classification is utilized, and fully connected layers are added for regression. The layers consist of two components with the same number of nodes as the classifier.

The SOH prediction result is illustrated in Fig.7. This shows that the model achieved high accuracy on the test set, with an R^2 value of 0.9768. The finding indicates that the convolutional layers did not learn solely for a single task but rather captured crucial capacity degradation information from time-series image data. The suggested approach demonstrates the potential for integrated battery condition assessment, facilitating the execution of multiple tasks.

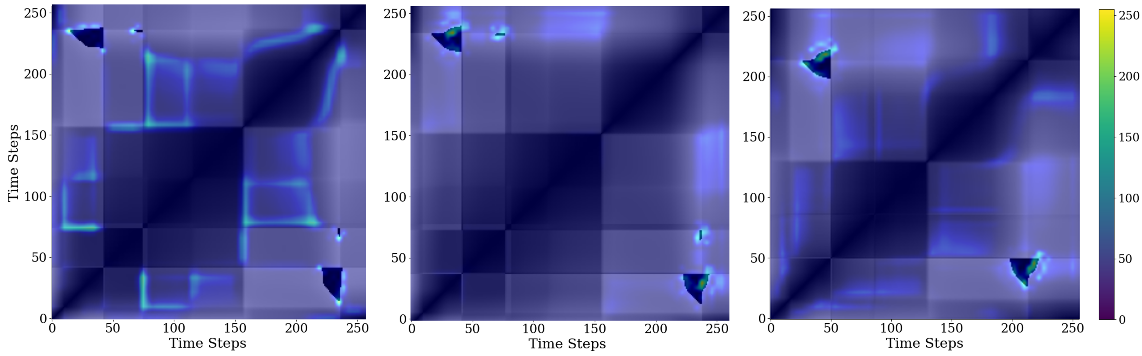

(a) (b) (c)

Fig. 6. Grad-CAM analysis for the b1c24 cell. (a) cycle 100 (class 0). (b) cycle 650 (class 1). (c) cycle 1000 (class 2).

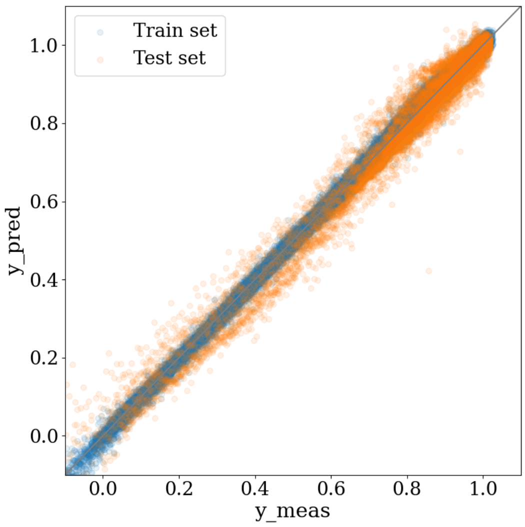

Fig. 7. SOH prediction result. train R^2: 0.9976, test R^2: 0.9768

4. CONCLUSION

In this study, we propose we propose a framework for monitoring battery status based on time-series image analysis. To accurately assess the operational state, we convert battery cycle data into images using the RP method. These images are then used to train a CNN model for knee classification, facilitating the preemptive detection of deterioration. A comparison with a time-series model highlights the potential of this approach for improved generalization.Grad-CAM analysis provides further insights into the aging mechanism by visualizing key regions that influence predictions. Additionally, SOH prediction using the pre-trained CNN model achieves high accuracy, demonstrating the applicability of this method beyond classification tasks. The results demonstrate the effectiveness of image transformation in battery health assessment and suggest the need to explore different transformation techniques. Future research will integrate self-supervised learning to enhance state prediction and improve the adaptability of the model under different conditions.

REFERENCES

Attia, P.M., Bills, A., Planella, F.B., Dechent, P., Dos Reis, G., Dubarry, M., Gasper, P., Gilchrist, R., Greenbank, S., Howey, D., et al. (2022). “knees” in lithium-ion battery aging trajectories. *Journal of The Electrochemical Society*, 169(6), 060517.

Eckmann, J.P., Kamphorst, S.O., Ruelle, D., et al. (1995). Recurrence plots of dynamical systems. *World Scientific Series on Nonlinear Science Series A*, 16, 441–446.

Fermín-Cueto, P., McTurk, E., Allerhand, M., Medina-Lopez, E., Anjos, M.F., Sylvester, J., and Dos Reis, G. (2020). Identification and machine learning prediction of knee-point and knee-onset in capacity degradation curves of lithium-ion cells. *Energy and AI*, 1, 100006.

Garcia, G.R., Michau, G., Ducoffe, M., Gupta, J.S., and Fink, O. (2022). Temporal signals to images: Monitoring the condition of industrial assets with deep learning image processing algorithms. *proceedings of the institution of mechanical engineers, part O: journal of risk and reliability*, 236(4), 617–627.

Greenbank, S. and Howey, D. (2021). Automated feature extraction and selection for data-driven models of rapid battery capacity fade and end of life. *IEEE Transactions on Industrial Informatics*, 18(5), 2965–2973.

Mallat, S.G. (1989). A theory for multiresolution signal decomposition: the wavelet representation. *IEEE transactions on pattern analysis and machine intelligence*, 11(7), 674–693.

Ren, L., Dong, J., Wang, X., Meng, Z., Zhao, L., and Deen, M.J. (2020). A data-driven auto-cnn-lstm prediction model for lithium-ion battery remaining useful life. *IEEE Transactions on Industrial Informatics*, 17(5), 3478–3487.

Severson, K.A., Attia, P.M., Jin, N., Perkins, N., Jiang, B., Yang, Z., Chen, M.H., Aykol, M., Herring, P.K., Fraggedakis, D., et al. (2019). Data-driven prediction of battery cycle life before capacity degradation. *Nature Energy*, 4(5), 383–391.

Sohn, S., Byun, H.E., and Lee, J.H. (2022). Two-stage deep learning for online prediction of knee-point in li-ion battery capacity degradation. *Applied Energy*, 328, 120204.

Zhang, L., Ji, T., Yu, S., and Liu, G. (2023). Accurate prediction approach of soh for lithium-ion batteries based on lstm method. *Batteries*, 9(3), 177.

Zhang, Y., Xiong, R., He, H., and Pecht, M.G. (2018). Long short-term memory recurrent neural network for remaining useful life prediction of lithium-ion batteries. *IEEE Transactions on Vehicular Technology*, 67(7), 5695–5705.